

RESEARCH ARTICLE

Influence of Debris Size on the Tribological Performance of Flame-Sprayed Coatings

Riyadh A. Al-Samarai¹, Abdulsalam Y. Obaid^{2*} and Y. Al-Douri^{3,4}

¹Electromechanical Engineering Department, Engineering College, University of Samarra, Samarra, 34010, Iraq

²Engineering Affairs Department, University of Fallujah, Iraq

³Department of Mechanical Engineering, Faculty of Engineering, Piri Reis University, EflatanSk. No:8, 34940 Tuzla, Istanbul, Turkey

⁴Nanotechnology and Catalysis Research Centre, University of Malaya, 50603 Kuala Lumpur, Malaysia

ABSTRACT – Due to the increased contact pressure and abrasive action on the coated surface, larger debris particles can result in higher wear rates. When designing and applying flame spray coatings in various industrial environments, it is important to consider how debris size affects the frictional performance of the coatings. This work aims to assess debris particle size's effect on Ni-based alloy coating's tribological properties. This is a key manufacturing issue that can help prolong the life of devices and provide proper maintenance. Debris is rated as Al₂O₃ solid particles, where their size ranges from 1.5 ± 0.03 μm to 42 ± 0.03 μm, dispersed in an oil lubricant. The coatings are characterized using scanning electron microscopy (SEM) and atomic force microscopy (AFM), while the cross-sectional evaluation is analyzed utilizing X-ray Diffraction (XRD). The coating is sprayed with NiCrBSi and melted in a flame. Hardened F-5220 metal forms a counter disk (according to ASTM A681). Our findings demonstrate that the alumina particles cause wear to increase significantly, particularly for bigger particles. When it comes to micrometer-sized particles, an increase in volume loss is seen as a result of increased surface roughness, plenteous microgrooves, and plastic flow of the NiCrBSi coating vertically to the sliding orientation. In addition, it has been proven that the nanosized particles play a secondary role in a tribological system in contrast to microparticles. Debris measurement is quantitatively related to friction and lubrication adjustments. Surface roughness can be assessed as a characteristic of the particle size. Large particles cause excessive induce high coefficient of friction at NiCrBSi coatings.

ARTICLE HISTORY

Received : 29th Aug. 2023

Revised : 13th Aug. 2024

Accepted : 17th Sept. 2024

Published : 22nd Nov. 2024

KEYWORDS

Tribology

Roughness

Debris size

NiCrBSi coatings

1. INTRODUCTION

In the automotive and aviation industries, internal components have been coated with mating surface treatments and lubricants to reduce the effects of tool wear [1,2]. Lubricant manufacturers have developed the basic characteristics of friction and wear and discovered the behavior of lubricating oil vapors, where the lubricating properties can determine the thickness of the lubricating film. [2-4]. Friction and wear are reduced if the lubricating oil layer prevents physical contact between rough surfaces. This is called hydrodynamic lubrication. However, objects usually work under excessive loads, pressures, and temperatures, which may lead to contact with rough surfaces at some point. Therefore, working agents usually work in a mixed lubrication mode. Wear resistance plays an important role in the industrial use of objects [4-8]. When the surfaces come into contact, the particles contaminating the lubricating medium are scraped off by solid particles suspended in the lubricating oil, known as fines, which is one of the most important problems in the industry. In addition to particles generated internally, lubricating oil may be contaminated with various particles from the environment, such as those often found in automobile engines. The problem of external particles is acute in engineering [8-10]. The study of wear resistance methods for computing units and formulations of lubricating oils contaminated with abrasive materials is of great importance [10].

Particles in the lubricating environment have been well studied since it is very important to consider the wear phenomenon. Therefore, the condition-based positioning strategy uses the relationship between the particle size, type, and structure in the aspect of location [11-13]. Maintenance is important to maintain and improve the normal overall performance of objects operating at high speed [14]. To summarize the relationship between equipment and particle size, since it is specific to each case, large and coarse particles can usually enter the gearbox [15]. Many failure studies (gearboxes, motors, gears, etc.) have confirmed that the particle size increases with time until the desired failure [16-18]. The computing system is subjected to extreme loads and requires intervention to avoid failure [19]. The lubricating oil in the environment will increase the amount of force required to engage the mating components, causing additional wear due to particle plowing. These results become more extreme under excessive stress and speed limitations such as housing rotation [20,21]. However, studies show that additional particles are found under acceleration conditions [22]. Thus, some studies [23,24] suggested that the formation of triple layers by particles can reduce friction and create a protective layer. Smaller debris particles with a perfectly spherical shape can act as nano- or micro-carriers, distributing the load between the contacting surfaces. At low pressure, the temperature increases due to a sharp increase in the hydrodynamic stress

between the contacting surfaces (“sliding effect”). Thus, an assessment of the current literature shows that the effect of particles on friction depends on the friction conditions [25]. For a machine whose surface roughness is constant, it is reasonable to take this into account. However, it is proposed that true roughness be used to study frictional behavior that eventually fails. Unlike the original roughness, the new parameter introduced in this paper is mainly based on true roughness. Using highly abrasive particles that make the particles harder than the mating surfaces, the objective is to investigate how particle size affects the frictional properties of nickel-based coatings. To evaluate the effect of size, three different particle sizes of aluminum oxide ranging from $0.15 \pm 0.03 \mu\text{m}$ to $42 \pm 0.03 \mu\text{m}$ were added and distributed in lubricating oil. It should be noted that most studies show that the presence of larger particles is an indication of increased friction and wear, mainly at low pressure. Some field results showed that the presence of debris resulted in decreased friction. Accordingly, other studies claim that the presence of debris can lead to the formation of three layers that cause an insulating layer and thus reduce friction [11]. Kim et al. [12] investigated the abrasive wear and dry sliding on components and the wear resistance of these coatings. The maximum quality was shown by a 35% WC coating with NiCrBSiC. (Higher hardness and lower porosity). However, the addition of 25% WC tungsten carbide powder showed that the addition of 40% WC provided better wear resistance in the DSRW (dry sand wheel) wear test, while the sugar wear test showed better wear resistance. Understanding the effect of particle size on the tribological performance of flame-sprayed coatings is important for improving the performance, durability, and efficiency of these coatings. The knowledge gained can lead to improved materials, cost savings, improved maintenance strategies, and advances in coating technology in various industries. In this work, highly abrasive particles are used to simulate the best conditions where the fragments are stronger than the contact surfaces and have an irregular shape. Different sizes (nano size), $(0.15 \pm 0.03 \mu\text{m})$, $(34 \pm 0.03 \mu\text{m})$, and $(42 \pm 0.03 \mu\text{m})$ show the dispersion of Al_2O_3 particles used as a waste source in our test.

2. EXPERIMENTAL PROCEDURE

2.1 Materials and Methods

The size of the selected particles ranges from 15 to 42 microns and they have a well-defined spherical shape. Their melting point is $1025 \text{ }^\circ\text{C}$. As shown in Figure 1, these particles are used for coating. Understanding the key powder properties that will affect the coating process and the quality of the final coating requires understanding the NiCrBSi coating powder in its original morphology, as shown in the SEM image in Figure 1. The coating performance can be improved by predicting and optimizing the powder behavior during deposition by studying the particle shape, size distribution, surface texture, and uniformity. This detailed explanation highlights the importance of the original powder morphology in obtaining high-quality NiCrBSi coatings. Figure 2 shows the micrometer-sized Al_2O_3 particles imaged by a scanning electron microscope (SEM, JXA840), which examines their different sizes and shapes.

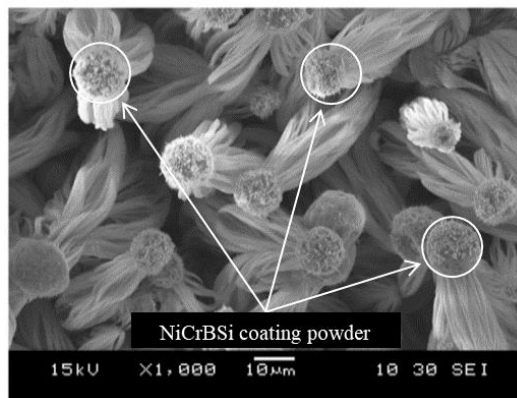


Figure 1. SEM of NiCrBSi coating powder at initial morphology

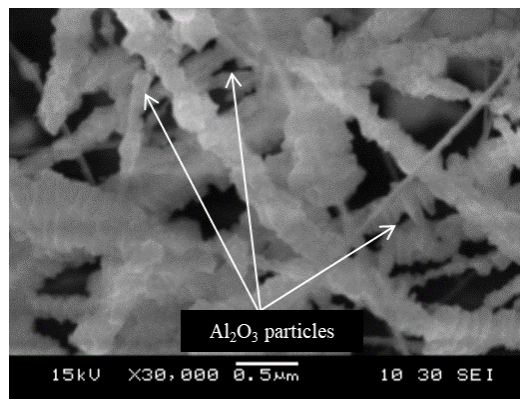


Figure 2. SEM morphology and distribution of Al_2O_3 particles used in the process.

Table 1. Parameters of thermal spray

Torch Speed (mm/s)	No. of strokes	Distance (mm)	Acetylene Pressure (bar)	Oxygen Pressure (bar)	Air pressure (bar)	Flame type
65.5	7	142	0.65	5	3.5	Neutral

Particles of Al₂O₃ (ALO PRAXAIR-101), Al₂O₃ (ALO-325 mesh) and Al₂O₃ (NANOX S2600S). In 10 ml of lubricating oil, the particles are uniformly distributed. Verification analyses are carried out using only lubricating oil. The NiCrBSi coating (M-772.33) is a self-flowing alloy (starts as a powder) and has the following chemical composition: 3.52% Si, 0.3% C, 1.7% B, 7.71% Cr and 2.66% Fe. Relaxation. The substrate material is wet sand. Distribution of Al₂O₃ particles used as a source of debris. The ASTM G 99 test is used for cylindrical pins with a diameter of 5 mm and a length of 15 mm. A counting disk is used to check the pin on the disk, the pins are made of AISI 304 steel.

Before spraying, the surface of the web is ground with 99.77% pure abrasives to obtain a smooth and even base surface, onto which the NiCrBSi coating is applied using a Castolin Eutectic CDS-8000 spray gun. The most important parameters are listed in Table 1. An oxyacetylene cutter with a temperature of 1035 °C and a measuring speed of 150 mm/min is used to coat the web after spraying. The coating thickness is about 1.20 µm with a total roughness of Ra = 0.018 µm.

2.2 Tribology Tests and Lubricating

Tribological studies are carried out using a pin on disc tribometer (TE79/P) at T = 27 °C and humidity ~ 65%. Mineral oil per minute is 8 drops from (CUT-MAX 5-20) with a viscosity equal to 100 ± 0.1 cSt at 44 °C and a density equal to 0.780 g/cm³. Each of the friction checks is usually performed below a starting speed of 0.035 m/s, and it increases every 5 minutes (22 m) in a stepwise manner; 0.084, 0.120, 0.155, 0.191. The load is 10 to 30 N.

The equation for calculating a specified wear rate:

$$\text{Volume loss} = V = A \times H \text{ (mm}^3\text{)} \quad (1)$$

where, A = Cross-sectional area, H = Average height loss

$$\text{Sliding Distance} = V \times T \text{ (m/s) where } V = \text{Velocity(m/s), } T = \text{Time (min)} \quad (2)$$

$$\text{Sliding Velocity} = \frac{2 \times \pi \times N \times r}{60 \times 1000}, \text{ where } N = \text{rpm, } r = \text{Track radius in mm} \quad (3)$$

$$\text{Wear rate} = \frac{\text{Volume Lost}}{\text{Sliding Distance}} \text{ (mm}^3\text{/mN)} \quad (4)$$

$$\text{Specific wear rate (SWR.)} = \frac{\text{Wear rate}}{\text{Normal Load}} \text{ (in mm}^3\text{/mN)} \quad (5)$$

3. RESULTS AND DISCUSSION

The tribological performance of flame-sprayed coatings is significantly affected by debris size. While larger particle sizes contribute to increased wear rates and surface degradation, smaller debris sizes typically improve performance by reducing friction and wear. These findings provide insightful advice for optimizing coating applications in practical environments.

3.1 Characterization of Surface

The study of the topographic, chemical, and physical properties of a material's surface is known as surface characterization. It is important to understand how surface properties affect service life, utility, and performance in various applications. Surface characterization is a fundamental procedure that sheds light on the properties and behavior of materials in various applications. Engineers and scientists can select better materials, improve manufacturing processes, and enhance product performance by understanding surface properties.

3.1.1 SEM topography

Figure 3 shows the scanning electron microscope (SEM) images of three sizes (0.15 ± 0.03 µm), (34 ± 0.03 µm), and (42 ± 0.03 µm) depicting the dispersion of Al₂O₃ particles used as a debris source. It depicts the surface of NiCrBSi, which has been transformed into very fine and widely spaced pits during oil lubrication. Our results show that the particle size has a significant effect on the surface roughness. The wear rate and friction coefficient increase sharply due to the change in surface roughness caused by the increase in particle size. The mechanism of NiCrBSi is Al₂O₃ nanowires with a thickness of +1.5 g (0.15-0.03 µm) with a large surface morphological variation. Figure 5 shows the surface morphology after tribological evaluation at a distance of 550 m. There are morphological differences depending on the Al₂O₃ particle size. The characterization is performed using scanning electron microscopy on worn surfaces to determine the effect of Al₂O₃ particles on the NiCrBSi coating. The sample is coated with NiCrBSi and the determined profiles on the scars are confirmed after friction studies using oil only, oil + 1.5 g nm Al₂O₃ (0.15 ± 0.03 µm), oil + 1.5 g nm Al₂O₃ (34 ± 0.03 µm) and oil + 1.5 g nm Al₂O₃ (42 ± 0.03 µm). Al₂O₃ particles with a size of nm to 42 µm are used as dispersed in lubricating oil. The test

coating is created by flame deposition of NiCrBSi. These compositional elements can help prevent damage to the mating parts in preventive maintenance procedures. In addition, they can be very useful for determining the maximum service life of the rubbing parts. The layer thickness is limited, although the roughness increases to some extent. The nanowires with nano scratches and large morphological changes on the surface belong to the mechanism of NiCrBSi with a thickness of $+1.5 \text{ g}$ nanometers of Al_2O_3 ($0.15 \text{ }\mu\text{m}$) (see Figure 6). The traction of the compressed Al_2O_3 nanoparticles is probably responsible for the presence of plowing marks, which can be seen in Figure 5b. The surfaces treated with oil and Al_2O_3 with a thickness of $0.15 \text{ }\mu\text{m}$ are much rougher than the surfaces treated with oil and NiCrBSi. The typical roughness values of the nanoparticles under steady-state friction and speed are $0.036 \text{ }\mu\text{m}$, while the oil-treated NiCrBSi + Al_2O_3 sample is $0.054 \text{ }\mu\text{m}$.

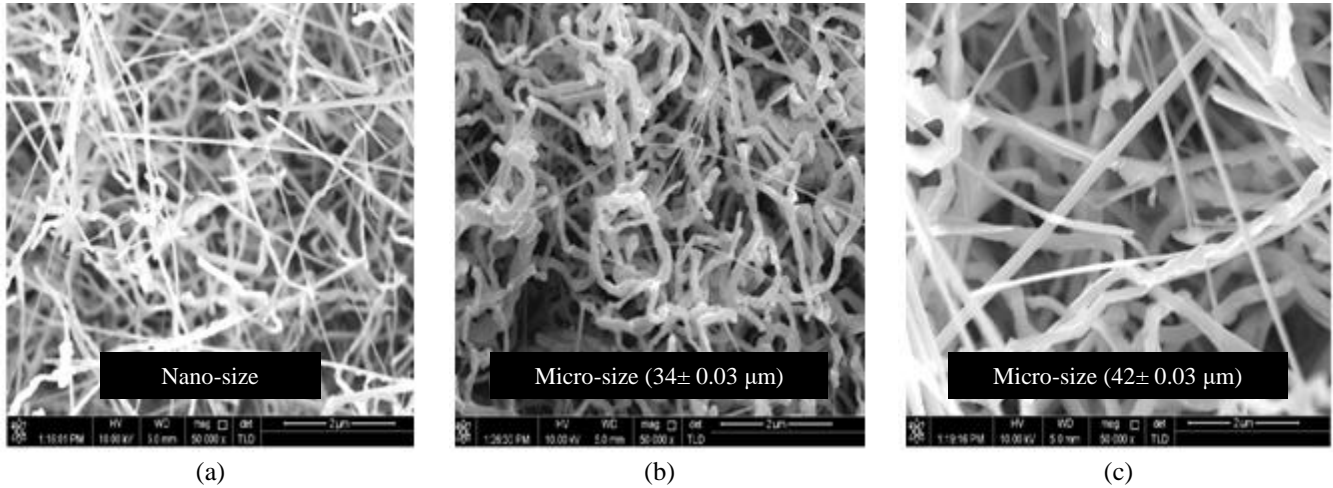


Figure 3. Al_2O_3 employed as a source of debris, SEM dispersion of the particles: (a) Nano-size, (b) Micro-size ($34 \pm 0.03 \text{ }\mu\text{m}$) and (c) Micro-size ($42 \pm 0.03 \text{ }\mu\text{m}$)

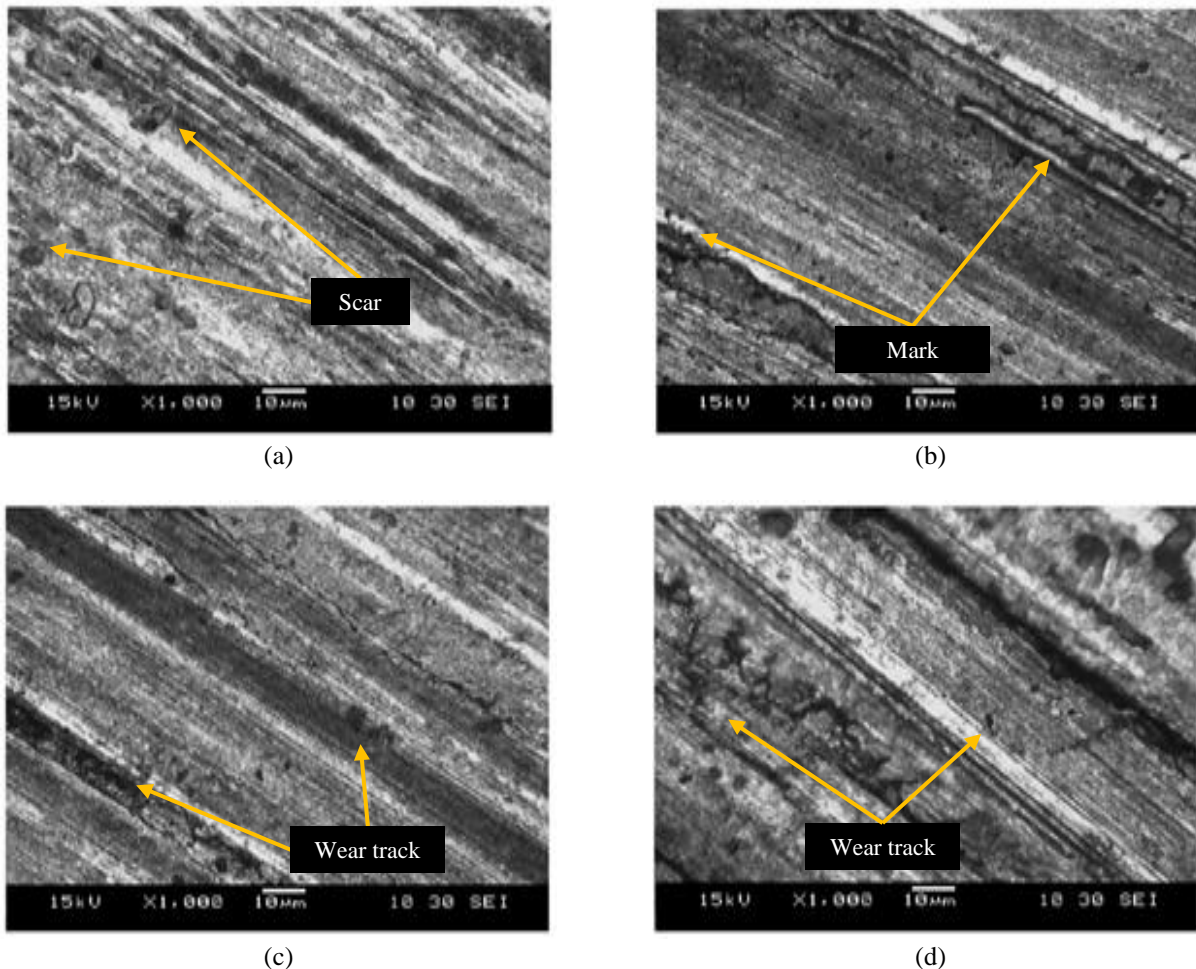


Figure 4. SEM of worn of NiCrBSi: (a) Only oil, (b) Oil + 1.5 g of nanometer Al_2O_3 ($R_a = 0.15 \pm 0.03 \text{ }\mu\text{m}$), (c) Oil+ 1.5 g micrometric Al_2O_3 ($R_a = 34 \pm 0.03 \text{ }\mu\text{m}$) and, (d) Oil + 1.5 g micrometric Al_2O_3 ($R_a = 42 \pm 0.03 \text{ }\mu\text{m}$)

The experiment with Al_2O_3 shows that the worn bottom contains a large number of plowing grooves, which are united by the deformation on the inflicted scars (Figure 7a). Fine cutting is dominant for the Al_2O_3 coating at $42\ \mu\text{m}$; in this case, larger plastic deformation and scratches are shown in Figure 7b. It shows the changes in the particle trajectory for the micro deformation of the coated surface. Typical roughness values for a 550 m trajectory are $0.525\ \mu\text{m}$ for $34\ \mu\text{m}$ Al_2O_3 and $1.85\ \mu\text{m}$ for $42\ \mu\text{m}$ Al_2O_3 . When placed between moving surfaces, the hard Al_2O_3 particles are free to rock. The wear methods used today are distinctive. The increased impact velocity of the smaller Al_2O_3 particles leads to microdeformation and scratches. Hard particles are deposited when using large Al_2O_3 particles, while medium and large Al_2O_3 particles produce micro deformations and scratches through impact and wear.

In addition, the spalling mechanism is fixed in each case. This is due to the interaction of the Al_2O_3 components and the abnormally fast decomposition of the NiCrBSi lining, as well as cutting, scratching, and micro deformations that change the trajectory of the particles during friction. Figure 6 (a, b) shows rolling along and along the entire length of the grooves. The grooves create the appearance of rolling. The grooves wear simultaneously, according to the test conditions. Moreover, high friction, which unintentionally mixes aluminum oxide particles with the lubricant, can cause microdeformations [26]. Reduced power sources, in most cases, have elastic-plastic deformations.

These deformations occur around the particles. In any case, the probability of collision with particles is higher, which leads to a transition from micro-plowing to micro-cutting [27]. The data obtained indicate that the presence of dispersed particles in the lubricant reduces the frictional efficiency of the process. This leads to an increase in the friction coefficient. The results also show that the amount of lubricant is limited by an increase in the particle size.

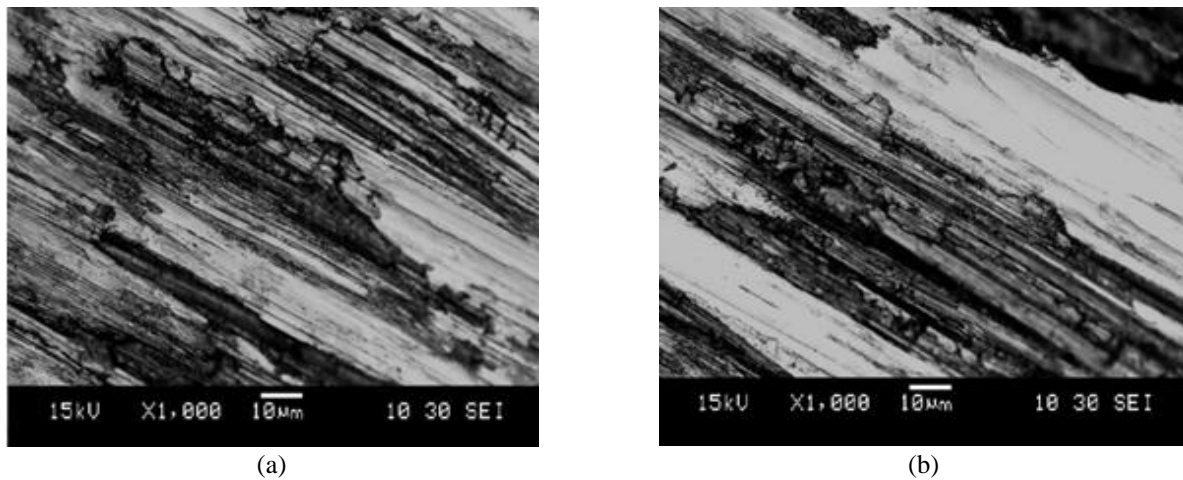


Figure 5. SEM of layer for NiCrBSi coating of grooves after 550 m: (a) Only oil & (b) Oil + 1.5 nanometers Al_2O_3

3.1.2 Worn surface

The roughness of the NiCrBSi coating for each Al_2O_3 particle size is shown in Figure 6. The perpendicular motion is recorded and the roughness parameters are calculated along the profile. The addition of 1.5 g nanometers Al_2O_3 ($1.5 \pm 0.03\ \mu\text{m}$), 1.5 g micrometers Al_2O_3 ($34 \pm 0.03\ \mu\text{m}$), and 1.5 g micrometers Al_2O_3 ($42 \pm 0.03\ \mu\text{m}$) to the lubricant yields roughness of 0.042, 0.510 and $1.55\ \mu\text{m}$, respectively [31]. A sensor (PLu 2300), which allows the extraction of 3D components, is used once to detect the NiCrBSi-coated samples during the test segment. Figure 5 shows the NiCrBSi coatings and deposited profiles, as well as the sliding distances up to 550 m.

The addition of oil resulted in a moderate exchange of deposited marks (Figure 4(b)) in contrast to the roughness (Figure 4(a)). The addition of 1.5 g Al_2O_3 particles ($0.15 \pm 0.03\ \mu\text{m}$) to the lubricated oil resulted in the formation of scratches, as shown in Figure 4c. After the addition of 1.5 g Al_2O_3 ($34 \pm 0.03\ \mu\text{m}$) and Al_2O_3 ($42 \pm 0.03\ \mu\text{m}$), grooves, excessive scratches, and extreme deformation were found at the bottom of the specimens (see Figures 4(c) and 4(d)). The empirical relationships between particle size and roughness, as well as between roughness and lubrication conditions, are evaluated. These joint qualities can facilitate preventive maintenance to protect the surfaces of mating components [25]. In addition, there are spherical aluminum oxide particles in the oil.

The lubricant may accidentally fall on the surface, which is divided by large particles due to the large particles, moderate rolling speed, and high kinetic energy of small particles. This may lead to microdeformations [26]. The addition of oil results in a moderate exchange of the deposited marks (Figure 7(b)) in contrast to the roughness (Figure 7(a)). The addition of 1.5 g Al_2O_3 particles ($0.15 \pm 0.03\ \mu\text{m}$) to the lubricant caused the formation of scars, as shown in Figure 4c. After the addition of 1.5 g Al_2O_3 ($34 \pm 0.03\ \mu\text{m}$) and Al_2O_3 ($42 \pm 0.03\ \mu\text{m}$), grooves, excessive scars, and extreme deformation were found at the bottom of the specimens (see Figures 6(c) and 6(d)). The purpose of the SEM and roughness data presented in Figure 6 is to conduct a thorough investigation of how different lubrication conditions affect the NiCrBSi coating surface after severe sliding wear. The focus is on comparing the effects of conventional oil and oil with different Al_2O_3 particle sizes on the base roughness, illustrating how particle size can either improve or deteriorate the frictional performance of the coating. Understanding which lubrication approach provides the best protection and wear resistance for NiCrBSi

coatings is based on this comparison in Figure 6 and the AFM topography of the coating that demonstrates the presence of the coating.

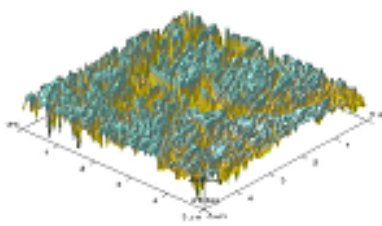
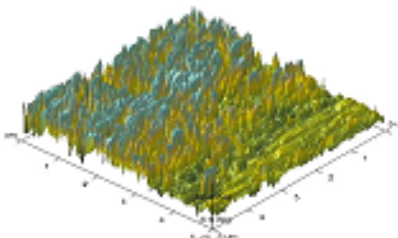
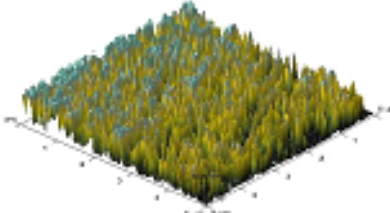
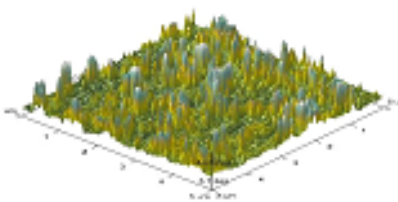
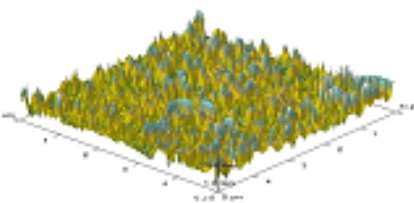
		Roughness results	
(a)		Image of Raw	Initial roughness
		Image of Mean	0.0054 μm
		Image of Z. Range	122 μm
		Image of Surface	28.4 μm
		Image. of Surface	27.0 μm
		Image of. Area Difference	30.3 %
		Image of Rq	17 μm
		Image of Ra	Initial roughness
		Roughness results	
(b)		Image of Raw.	1± 0.03 μm
		Image of Mean	0.0054 μm
		Image of Z. Range	128 μm
		Image of Surface.	31.4 μm
		Image. of Surface	29.0 μm
		Image of. Area Difference	30.3 %
		Image of Rq	28 μm
		Image of Ra	1± 0.03 μm
		Roughness results	
(c)		Image of Raw.	1.5± 0.03 μm
		Image of Mean	0.0054 μm
		Image of Z. Range	122 μm
		Image of Surface.	28.4 μm
		Image. of Surface	27.0 μm
		Image of. Area Difference	30.3 %
		Image of Rq	33 μm
		Image of Ra	1.5± 0.03 μm
		Roughness results	
(d)		Image of Raw.	34± 0.03μm
		Image of Mean	0.0054 μm
		Image of Z. Range	122 μm
		Image of Surface.	28.4 μm
		Image. of Surface	34.0 μm
		Image of. Area Difference	36.1 %
		Image of Rq	64 μm
		Image of Ra	34± 0.03μm
		Roughness results	
(e)		Image of Raw.	42± 0.03 μm
		Image of Mean	0.0054 μm
		Image of Z. Range	122 μm
		Image of Surface.	28.4 μm
		Image. of Surface	34.0 μm
		Image of. Area Difference	36.1 %
		Image of Rq	77μm
		Image of Ra	42± 0.03 μm

Figure 6. 2D-AFM Topography of roughness and SEM for NiCrBSi coating after 550 m; (a) Roughness (b) Solely oil (c) Oil + 1.5g nanometric Al₂O₃ (1.5± 0.03 μm) (d) Oil+ 1.5g micrometric Al₂O₃(34± 0.03μm) and (e) Oil +1.5g micrometric Al₂O₃ (42± 0.03 μm)

Experimental relationships between roughness and the lubrication regime as well as between particle size and roughness are evaluated. These relationship characteristics can be used for preventive maintenance to prevent damage to the surfaces of mating parts. Depending on the applied stress, mechanical properties, sliding speed, and size and shape of the contacting

surfaces, abrasive particles penetrate the coated surface at sharp angles. This penetration into the surface causes micro-plowing or micro-cutting depending on the angle of attack [26]. Scanning electron microscopy characterization of the worn surface pits revealed varying lines and degrees of rolling along the grooves, depending on the particle size. In friction experiments, it has been shown that NiCrBSi coatings strengthen particles trapped between moving surfaces due to cumulative plastic deformation resulting from repeated sliding and rolling of Al_2O_3 .

The strain hardening values of the NiCrBSi coating increase with any increase in Al_2O_3 particle size, and this appears to significantly increase the surface nano-indenting values. The results show that the friction performance of the system is significantly reduced by the presence of abrasive debris dispersed in the lubricating oil, and provide information on the expected remaining life of the friction elements.

3.2 Tribology Tests

To determine the general characteristics of the imprint depth in the coating, this is done with a minimum imprint depth of 2 microns. At least 20 measurements are made at the sites and common values are taken into account in this information. 130 mm between the gun and the substrate. Initially, the imprint is 135 mm between the gun and the substrate. Table 2 shows an alternative procedure for NiCrBSi, which is related to the changes in processes and topography after friction testing of NiCrBSi coatings. The lubricant is micrometrically saturated with Al_2O_3 to obtain the lowest nanoindent results. This may also be a result of plastic deformations due to the use of micrometric Al_2O_3 , an increase in residual compressive stress at high loads, and an improvement in hardening caused by higher particle pressure [27].

SEM characterization of the particle-based etching reveals abrasive grooves and varying degrees of wear at specific stages of the grooves. Post-friction nano-dent analysis supports the hypothesis that the NiCrBSi coatings harden as a result of cumulative plastic deformation caused by the Al_2O_3 particles repeatedly being trapped between surfaces and rolling and sliding. The hardness values of the NiCrBSi coatings increase with increasing Al_2O_3 particle size, and this is expected to have a significant effect on how easily the coatings flex.

Table 2. After 550 meters, nanoindentation of the surface of the NiCrBSi coating and modulus of elasticity

Solely oil	Oil+ nanometric Al_2O_3 ($0.15 \pm 0.03 \mu\text{m}$)	Oil+ micrometric Al_2O_3 ($34 \pm 0.03 \mu\text{m}$)	Oil+ micrometric Al_2O_3 ($42 \pm 0.03 \mu\text{m}$)
Nanoindentation (GPa)	3.88	4.67	5.44
3.44			
Modulus of elasticity	193	198.5	202.4
137.33			

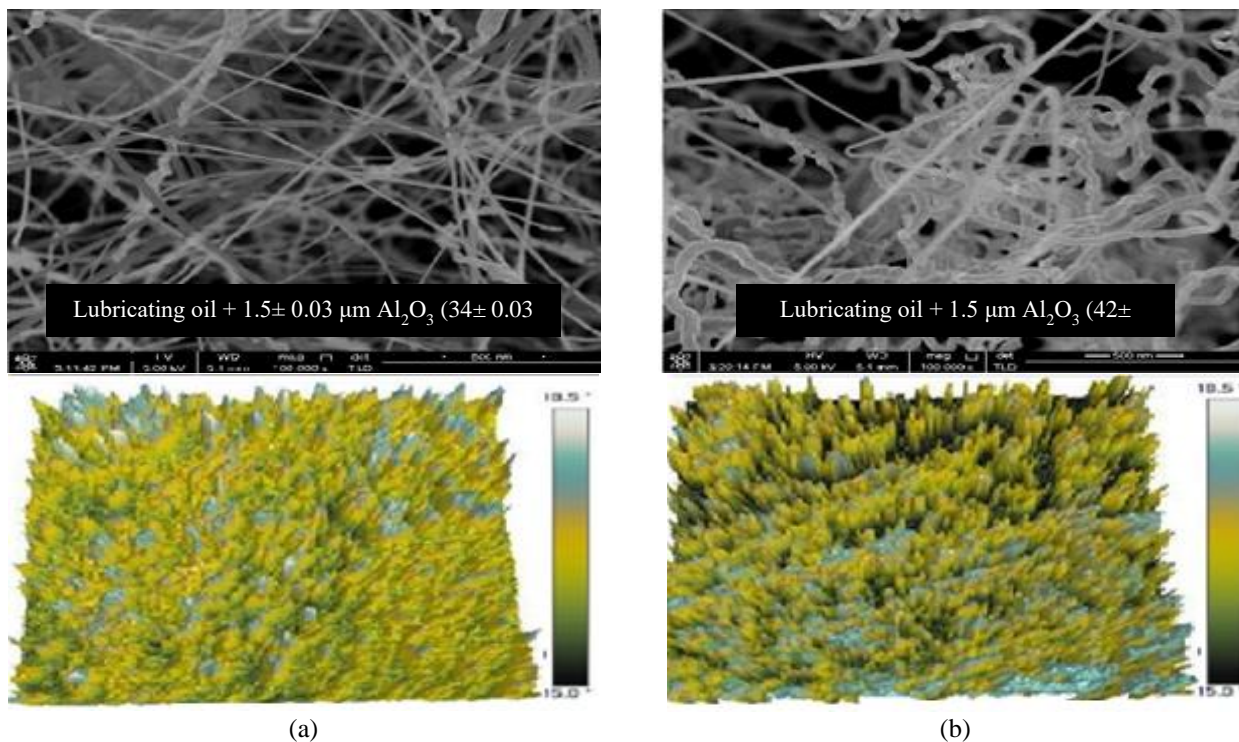


Figure 7. SEM and AFM of worn: (a) Lubricating oil + $1.5 \pm 0.03 \mu\text{m} \text{Al}_2\text{O}_3$ ($34 \pm 0.03 \mu\text{m}$), (b) Lubricating oil + $1.5 \mu\text{m} \text{Al}_2\text{O}_3$ ($42 \pm 0.03 \mu\text{m}$)

3.3 Friction Coefficient

The friction coefficient values after the tribological evaluations are shown in Figure 8. The obtained data show that the presence of Al_2O_3 particles significantly affects the interaction between the friction coefficient and roughness. There is a complex relationship between surface roughness and friction coefficient as shown in Figure 8. The friction coefficient reaches its maximum (1.2-2.3) depending on different surface roughness. However, the friction coefficient values of Al_2O_3 are higher at $33.2 \mu\text{m}$ and $38 \mu\text{m}$ because larger particles have smaller interfaces and limit close contact. This, in turn, will increase the applied pressure and hence increase the friction coefficient. Previous studies [29, 30] assumed rolling dominance when the friction coefficient is in the range of $\mu = 0.24$ to $\mu = 0.32$. The friction of fine-particle abrasives occurs at excessive and low speeds with friction coefficient values in the range $\mu = 0.225$ (Al_2O_3 particle size is $34 \pm 0.03 \mu\text{m}$) to $\mu = 0.266$ (Al_2O_3 particle size is $42 \pm 0.03 \mu\text{m}$). Under the preconditions of excessive contact (speed and contact stress), a significant increase in the friction coefficient occurs when the thickness of the lubricant layer is much smaller than the thickness of the Al_2O_3 particles. When the particle is used as a debris source, the friction coefficient has a characteristic structure. Two additional/specific reasons for the low friction coefficient when using nanoparticles were found: (1) the geometry of the contact area is minimal in the case of nanoparticles, and (2) particle contamination can reduce the harmful effects of nano-abrasive particles on the process [31].

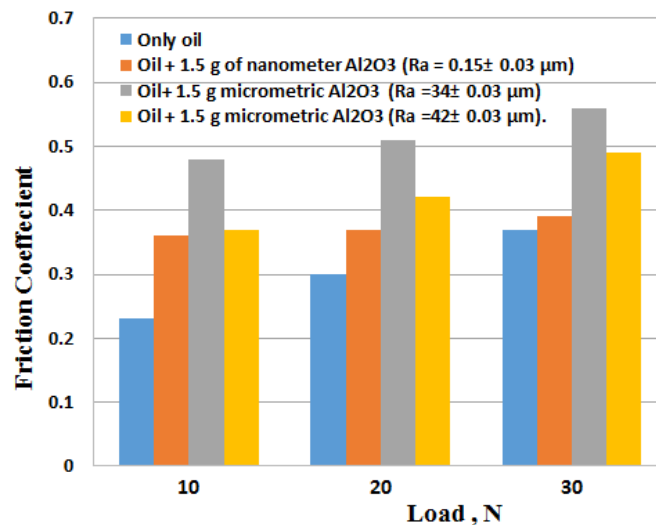


Figure 8. Changes in friction coefficient with roughness of worn surface (R_a) of test specimens

3.4 Wear Behavior

The size decreases only due to the contact of the previously reduced NiCrBSi oil + 1.5 g nm Al_2O_3 ($0.15 \pm 0.03 \mu\text{m}$) in contrast to the screw, which is still lubricated with + 1.5 g nm Al_2O_3 ($34 \pm 0.03 \mu\text{m}$), and the oil of 1.5 g nm Al_2O_3 ($42 \pm 0.03 \mu\text{m}$) at all speeds studied (Figure 9). At 550 m, the loss of 1.5 g nm Al_2O_3 lubricant is more than eight times greater than the loss in the screw due to oil alone. Thus, it is likely that the nm Al_2O_3 particles present in the lubricant are first detected in the softer NiCrBSi coatings, resulting in a contact abrasive. On the other hand, the results show that, unlike microparticles, nanoparticles can have little effect on the triboelectric process. The information on nanopores confirms that NiCrBSi coatings harden under stress due to cumulative plastic deformation that occurs with some sliding and rerolling ratio. Al_2O_3 particles get stuck between the rolling surfaces. With micrometric particles, larger roughness, micro-groove, and plastic surface of the NiCrBSi coating can be observed perpendicular to the sliding, resulting in large volumetric losses. The effects of plowing and rolling wear with micrometric Al_2O_3 also negatively affect the NiCrBSi pin coating (Figure 9). In the case of nano-sized Al_2O_3 oil + grease, a portion of the Al_2O_3 particles penetrates the smooth layer of the NiCrBSi coating, while the captured surfaces and the first sliding surfaces are immediately removed, thus agglomerating. This behavior affects the prevailing values due to the complex nanoparticles of aluminum oxide and penetration into a fairly soft Ni-Cr matrix will increase the nano-dent and reduce the damage caused by penetration of abrasive and nanoparticles of aluminum oxide with sharp edges [28]. The average experimental facts show the unusual particle sizes after a distance of 550 m (see Figure 9). This can be solved by increasing the electro-kinetic energy of the particles, which will lead to a decrease in the roughness rate. Serious sliding problems arise between the contacting surfaces due to excessive load and speed. The relationship is somewhat complicated when the disturbance between the surfaces is too large due to the accelerated load and speed, the contact becomes unstable and particles form from time to time, which leads to increased wear [31].

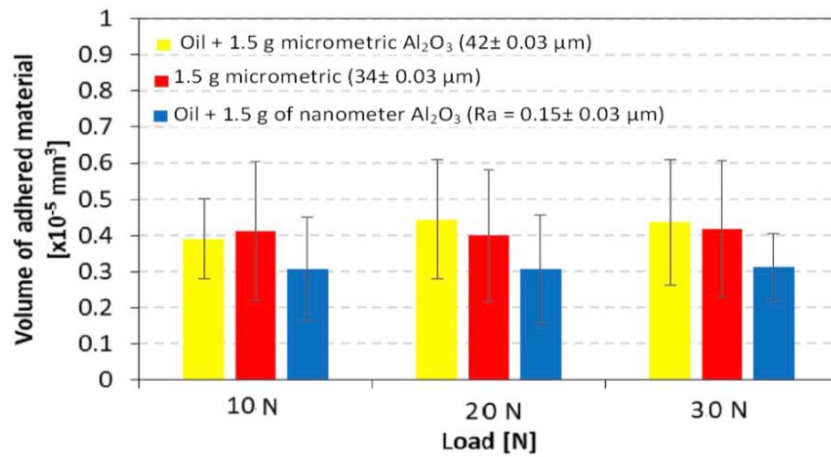


Figure 9. Wear volume of NiCrBSi coating at different loads and speeds depending on sliding distance (550 m)

4. CONCLUSIONS

The friction properties of the sprayed plasma were influenced by the experimental relationships between surface roughness and debris size. The results of the study can be summarized as follows:

- The experimental relationships between particle size and roughness, as well as roughness and the lubrication system, were evaluated. These relationships can help in preventive maintenance to avoid damage to the surfaces of mating parts. The lubricating oil caused a deterioration in the overall frictional performance of the process, which led to a significant increase in the friction coefficient with increasing speed, as well as in different lubricants.
- As a result of repeated sliding and rolling of Al₂O₃ particles between moving surfaces, scanning electron microscopy examination of the grooves revealed the presence of an abrasive layer with varying degrees of wear. The increase in Al₂O₃ particles contributes to the increase in the hardness values of the NiCrBSi coating.
- The experiments also showed that nanoparticles play a secondary role in the friction system, unlike microparticles. The size of the debris particles was quantitatively related to changes in friction and lubrication. Surface roughness can be evaluated as a characteristic of the size of the accumulated particles. Large particles caused an excessively high coefficient of friction in NiCrBSi coatings.

ACKNOWLEDGEMENT

The authors would like to thank the Department of Mechanical Engineering at Tikrit University for providing laboratory support and materials to perform the experiments.

CONFLICT OF INTEREST

The authors declare that they do not have any conflict of interest.

AUTHORS CONTRIBUTION

Riyadh A. Al-Samarai : Design concept, data collection, and interpretation of results

Abdulsalam Y. Obaid : Experimental work and analysis

Y. Al-Douri : Co-supervised the draft manuscript preparation

REFERENCES

- [1] J.D.J. Lozoya-Santos, J.C. Tudon-Martinez, R. Morales-Menendez, O. Sename, A. Spaggiari and R. Ramírez-Mendoza, "A general modeling approach for shock absorbers: 2 Dof Mr Damper case study," *Frontiers in Materials*, vol. 7, p. 590328, 2021.
- [2] S.W.R. Duym, "Simulation tools, modelling and identification, for an automotive shock absorber in the context of vehicle dynamics," *Vehicle System Dynamics*, vol. 33, pp. 261–285, 2000.
- [3] M. Shams, R. Ebrahimi, A. Raoufi and B. J. Jafari, "CFD-Fea analysis of hydraulic shock absorber valve behavior," *International Journal of Automotive Technology*, vol. 5, pp. 615–622, 2007.
- [4] N. Lavanya, P. Rao And M. Reddy, "Design and analysis of a suspension coil spring for automotive vehicle," *International Journal of Engineering Research and Applications*, vol. 9, pp. 151-157, 2014.
- [5] L. Dai, M. Chi, H. Gao and J. Sun, "An investigation into the modeling methodology of the coil spring," *Hindawi Shock and Vibration*, vol. 2020, no. 1, p. 8814332, 2020.
- [6] M. Wittek, D. Gąska, B. Łazarz and T. Matyja, "Coil springs in passenger cars – general theoretical principles and structural requirements," *The Archives of Automotive Engineering*, vol. 7, no. 2, pp. 141-159, 2016.

- [7] H.B. Pawar, A.R. Patil and S.B. Zope, "Design and analysis of a front suspension coil spring for three wheeler vehicle," *International Journal Of Innovations In Engineering Research and Technology*, vol. 3, pp. 1-10, 2016.
- [8] N. Singh, "General review of mechanical springs used in automobiles suspension system," *International Journal Of Advanced Engineering Research and Studies*, vol. 115, p. 122, 2013.
- [9] M. Rahman and S.B. Abdullah, "Numerical and experimental study on optimization of coil springs used in vehicles' suspension system," *Journal Of Engineering Advancements*, vol. 2, pp. 169-174, 2021.
- [10] C. Wei, Z. Wang, and J. Chen, "Sulfuration corrosion failure analysis of Inconel 600 alloy heater sleeve in high-temperature flue gas," *Engineering Failure Analysis*, vol. 135, p. 106111, 2022.
- [11] G. Li, G. Wang, J. Dong, W. Yeh, and K. Li, "DLEA: A dynamic learning evolution algorithm for many-objective optimization," *Information Sciences*, vol. 574, pp. 567-589, 2021.
- [12] M. Prem Kumar, N. Arivazhagan, C. Chiranjeevi, Y. Raja Sekhar, N. Babu, and M. Manikandan, "Effect of molten binary salt on Inconel 600 and Hastelloy C-276 superalloys for thermal energy storage systems: A corrosion study," *Journal of Materials Engineering and Performance*, vol. 33, no. 17, pp. 9070-9083, 2023.
- [13] M. Kuruba, G. Gaikwad, J. Natarajan, and P.G. Koppad, "Effect of carbon nanotubes on microhardness and adhesion strength of high-velocity oxy-fuel sprayed NiCr-Cr₃C₂ coatings," *Proceedings of the Institution of Mechanical Engineers, Part L: Journal of Materials: Design and Applications*, vol. 236, pp. 86-96, 2022.
- [14] X. Zhu, C. Zhong, and J. Zhe, "Lubricating oil conditioning sensors for online machine health monitoring—A review," *Tribology International*, vol. 109, pp. 473-484, 2017.
- [15] H. Wang, Y. Cheng, J. Yang, and Q. Wang, "Influence of laser remelting on organization, mechanical properties and corrosion resistance of Fe-based amorphous composite coating," *Surface and Coatings Technology*, vol. 414, p. 127081, 2021.
- [16] Jin, B.; Zhang, N.; Yin, S. "Strengthening behavior of AlCoCrFeNi(TiN) high-entropy alloy coatings fabricated by plasma spraying and laser remelting," *Journal of Materials Science & Technology*, vol. 121, pp. 163-173, 2022.
- [17] Al-Samarai, Riyadh A., and Yarub Al-Douri. "Surface protection from wear through coating," In *Friction and Wear in Metals*, pp. 135-173. Singapore: Springer Nature Singapore, 2024.
- [18] G. Li, R. Wu, X. Deng, L. Shen and Y. Yao, "Suspension parameters matching of high-speed locomotive based on stability/comfort pareto optimization," *Vehicle System Dynamics*, vol. 60, no. 11, pp. 3848-3867, 2022.
- [19] M. Čorić, J. Deur, L. Xu, H.E. Tseng and D. Hrovat, "Optimisation of active suspension control inputs for improved vehicle ride performance," *Vehicle System Dynamics*, vol. 54, no. 7, pp. 1004-1030, 2016.
- [20] A.S. Gad and E.-D. Samir, "Effect of optimal fuzzy models for pneumatic magnetorheological suspension system on ride performance under different conditions," *SAE International Journal of Vehicle Dynamics, Stability, and NVH*, vol. 6, pp. 421-440, 2022.
- [21] A. Shehata Gad, "Preview model predictive control controller for magnetorheological damper of semi-active suspension to improve both ride and handling," *SAE International Journal of Vehicle Dynamics, Stability, and NVH*, vol. 4, pp. 305-326, 2020.
- [22] Shehata Gad, S. Darakhshan Jabeen, and W. Galal Ata, "Damping magnetorheological systems based on optimal neural networks preview control integrated with new hybrid fuzzy controller to improve ride comfort," *SAE International Journal of Vehicle Dynamics, Stability, and NVH*, vol. 7, no. 4, pp. 1-24, 2023.
- [23] H. Han, B. Yim, N. Lee and Y. Kim, "Prediction of ride quality of a maglev vehicle using a full vehicle multibody dynamic model," *Vehicle System Dynamics*, vol. 47, no. 10, pp. 1271-1286, 2009.
- [24] G. Geetharamani, K. Dhinakaran, J. Selvaraj and S.C. Ezhil Singh, "Sport-utility vehicle prediction based on machine learning approach," *Journal of Applied Research and Technology*, vol. 19, pp. 184-193, 2021.
- [25] A. Khajepour and A. Soltani, "A coordinated control system for truck cabin suspension based on model predictive control," *International Journal of Heavy Vehicle Systems*, vol. 29, p. 518-536, 2022.
- [26] J. Liang, Y. Lu, D. Pi, G. Yin, W. Zhuang, F. Wang, J. Feng and C. Zhou, "A decentralized cooperative control framework for active steering and active suspension: Multi-agent approach," *IEEE Transactions on Transportation Electrification*, vol. 8, pp. 1414-1429, 2022.
- [27] Y. Al-Douri, R.A. Al-Samarai, S.A. Abdulateef, A.A. Odeh, N. Badi, and C.H. Voon. "Nanosecond pulsed laser ablation to synthesize GaO colloidal nanoparticles: Optical and structural properties," *Optik*, vol. 178, pp. 337-342, 2019.
- [28] T. Ghara, and P.P. Bandyopadhyay, "Understanding the role of in-flight particle temperature and velocity on the residual stress depth profile and other mechanical properties of atmospheric plasma sprayed Al₂O₃ coating," *Journal of the European Ceramic Society*, vol. 42, pp. 4353-4368, 2022.
- [29] A. Pattnayak, A. Gupta, N.V. Abhijith, D. Kumar, J. Jain, and V. Chaudhry, "Development of rGO doped alumina-based wear and corrosion resistant ceramic coatings on steel using HVOF thermal spray," *Ceramics International*, vol. 49, pp. 17577-17591, 2023.
- [30] B. Hou, H. Guo, N. Zhang, Q. Zhi, B. Wang, and J. Yang "Anisotropic friction derived from the layered arrangement of the oriented graphite flakes in the copper-iron matrix composite," *Tribology Letters*, vol. 78, pp. 1-13, 2022.
- [31] H. Torres, B. Podgornik, M. Jovičević-Klug, and M.R. Ripoll, "Compatibility of graphite, hBN and graphene with self-lubricating coatings and tool steel for high temperature aluminium forming," *Wear*, vol. 490, p. 204187, 2022.